From activation to stabilization

Different applications of a frustrated Lewis pair

Boom, D.H.A.

Chapter 4

Gold(I) Complexes of the Geminal Phosphinoborane *t*Bu$_2$PCH$_2$BPh$_2$

Abstract: In this work, we explored the coordination properties of the geminal phosphinoborane *t*Bu$_2$PCH$_2$BPh$_2$ (**2**) toward different gold(I) precursors. The reaction of **2** with an equimolar amount of the sulfur-based complex (Me$_2$S)AuCl resulted in displacement of the SMe$_2$ ligand and formation of linear phosphine gold(I) chloride **3**. Using an excess of ligand **2**, bisligated complex **4** was formed and showed dynamic behavior at room temperature. Changing the gold(I) metal precursor to the phosphorus-based complex, (Ph$_3$P)AuCl impacted the coordination behavior of ligand **2**. Namely, the reaction of ligand **2** with (Ph$_3$P)AuCl led to the heterolytic cleavage of the gold−chloride bond, which is favored over PPh$_3$ ligand displacement. To the best of our knowledge, **2** is the first example of a P/B-ambiphilic ligand capable of cleaving the gold−chloride bond. The coordination chemistry of **2** was further analyzed by density functional theory calculations.

Published in: *ACS Omega* **2018**, *3*, 3945−3951

4.1 Introduction

Ambiphilic ligands bearing a Lewis basic site for σ-donation and a Lewis acidic site for σ-acceptation have been recognized as ligands with unique coordination properties,[1] resulting in unusual bonding situations (Z-type interactions)[2,3] or halide abstraction from the metal precursor, which are both of interest for catalytic applications.[4,5] The coordination behavior of ambiphilic ligands has been extensively studied in combination with late transition metals, in particular, complexes with coinage metals. Among these coinage metals, gold(I) is the most explored and a plethora of gold complexes have been reported, which are mainly dominated by ligands bearing a Lewis basic phosphine, in combination with a variety of Lewis acidic sites based on boron,[6,7] aluminum,[8] gallium,[9] indium,[10] bismuth,[11] silicon,[12] tin,[12a] antimony,[13] zirconium,[14] and tellurium.[15]

In 2006, Bourissou and co-workers reported a bidentate phosphinoborane ligand that reacts with (Me_2S)AuCl to form complex **A** (Figure 1).[6a] In this example, the ambiphilic ligand reacts with the metal precursor by the displacement of the dimethyl sulfide ligand, resulting in the coordination of the phosphine to the gold(I) center. Interestingly, the solid-state structure of **A** revealed a Au−B distance of 2.66 Å, which is well within the sum of the van der Waals radii (∼3.9 Å), as well as slight pyramidalization of the boron center (Σ(CBC) = 355.8°), indicating a Z-type interaction between the gold(I) center and the Lewis acid. A year later, Bourissou and coworkers reported a tridentate phosphinoborane ambiphilic ligand, which can react with the same metal precursor also by the displacement of dimethyl sulfide to form complex **B** (Figure 1).[6b] The slightly distorted square planar coordination geometry forces the boron center in a closer proximity to the gold center (2.31 Å) compared to **A**, resulting in a stronger pyramidalization (Σ(CBC) = 341.2°), which suggests a stronger boron−gold interaction. To complete this family of phosphinoborane ligands with unique Z-type interactions, Bourissou and co-workers reported a tetradentate phosphinoborane (TPB) ligand that forms complex **C** (Figure 1) upon coordination to (Me_2S)AuCl.[6c] Dissociation of the gold−chloride bond was easily achieved by the addition of an external Lewis acid to **C**, giving rise to cationic (TPB)Au^+ species.[6d]

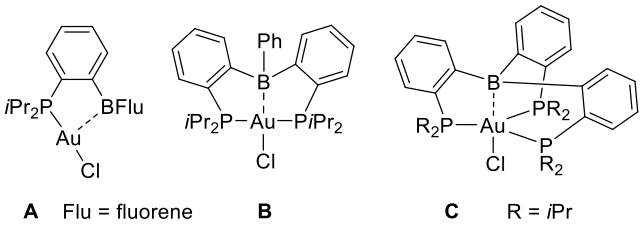

Figure 1. Ambiphilic ligand complexes of gold(I) chloride.

Interestingly, tri- and tetradentate phosphine-based ambiphilic ligands with heavier main-group Lewis acidic sites based on aluminum,[8c,d] gallium,[9] indium,[10] and silicon[12c] are reported to facilitate heterolytic Au−Cl bond cleavage without an additional halide abstracting agent. To date, phosphorus−aluminum ligand **1** is the only main-group-based bidentate ligand[14] that has been reported to perform this bond activation when reacted with tetrahydrothiophene gold(I) chloride ((THT)AuCl) forming zwitterionic complex **D** (Scheme 1),[8a,b] which proved to be an active catalyst for the cyclization of propargylamides in the absence of any additives. This demonstrates the potential of ambiphilic ligands as an alternative to silver salts for the activation of gold(I) precatalysts.[16]

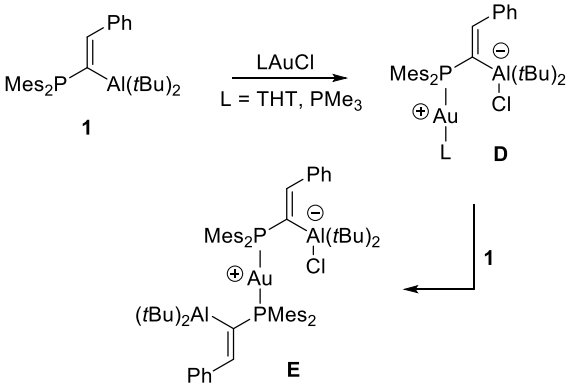

Scheme 1. Reactivity of **1** toward Au(I) precursors.

Recently, we developed ambiphilic phosphinoborane **2** which exhibits frustrated Lewis pair reactivity[17,18,19] when reacted with, for example, H_2, CO_2, isocyanates, alkynes, nitriles,

and nitrilium triflates,[20] but can also act as an ambiphilic ligand forming a luminescent complex upon coordination to Cu(I)Cl.[21] The related geminal P/Al-based FLP **1** and its capability to activate a gold−chloride bond inspired us to explore the coordination behavior of **2** toward gold(I) chloride complexes and also to study the underlying factors experimentally and computationally.

4.2 Results and Discussion

Reacting a solution of $(Me_2S)AuCl$ in dichloromethane (DCM) with 1 equiv of tBu$_2$PCH$_2$BPh$_2$ (**2**) resulted in the formation of two new species in solution, observed by $^{31}P\{^1H\}$ NMR spectroscopy at δ = 75.3 (major, 75%) and 80.5 (minor, 25%) and the formation of small amounts of insoluble purple solids (Scheme 2).[22] The X-ray diffraction analysis of colorless crystals obtained by vapor diffusion of *n*-pentane into a DCM solution confirmed the molecular structure of the major product **3**, in which ligand **2** has displaced the SMe_2 moiety, and in contrast to **1** (Scheme 1), did not cleave the gold−chloride bond.[23]

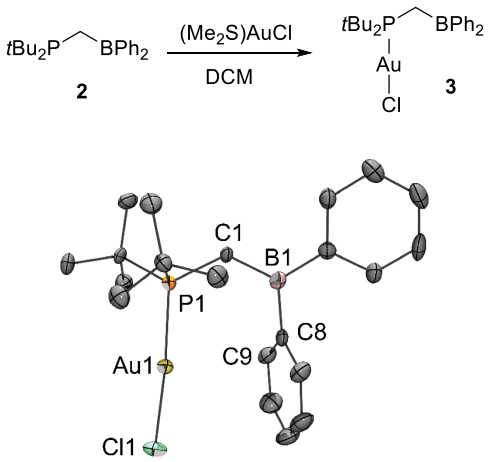

Scheme 2. Ligand displacement by Phosphinoborane **2** (top) and the molecular structure (bottom) of **3** (ellipsoids are set at 50% probability; hydrogens are omitted for clarity). Selected bond lengths (Å) and angles (°) for **3**: Selected bond lengths (Å) and angles (°): P1−Au1 2.2466(11), Au1−Cl1 2.2035(11), P1−C1−B1 119.8(3), B1−Au1 3.798(5), C8−Au1 3.262(4), C9−Au1 3.263(3), P1−Au1−Cl1, 174.35(4) Σ(CB1C) 359.8.

In the solid state, the P1−Au1−Cl1 bond angle is slightly bent (174.35(4)°)[24] and the P1−C1−B1 bond angle (119.8(3)°) is comparable to that of the optimized geometry[20a] of the free ligand (2.1° increase). The B1−Au1 distance of 3.798(5) Å is just within the sum of the van der Waals radii (~3.9 Å), however, the planar geometry of the boron center (Σ(CB1C) = 359.8°) is rotated away from the gold center (torsion angle P1−C1−B1−C8 = 46.4(5)°), making any Z-type interaction unlikely. Interestingly, one of the phenyl groups of the ligand is oriented in an almost parallel fashion to the metal chloride bond,[25] and the Au1−C8 and Au1−C9 bond distances of 3.326 Å indicate a possible weak π-interaction, comparable to those previously reported for Au(I) complexes bearing biarylphosphine ligands.[26,27] The $^{11}B\{^{1}H\}$ NMR spectrum showed one signal at 70.2 ppm, which is comparable to that of the free ligand (72.3 ppm)[20] and is indicative for a planar diarylalkylborane, supporting the absence of any Z-type interaction.

Analysis of compound **3** by density functional theory (DFT) calculations at the ωB97X−D/6-31G* (Def2-QZVP for Au) level of theory[28] revealed two possible conformers which are close in energy (**3** and **3′**, Figure 2). Conformer **3** was found to be the global minimum and closely resembles the geometry of **3** in the solid state as determined by single-crystal X-ray crystallography (Scheme 2). Interestingly, also a local minimum was found, albeit higher in energy (**3′**, $\Delta\Delta E$ = 1.4 kcal/mol). **3′** revealed a significantly more bent P1−C1−B1 backbone (106°) compared to **3** (119°), and the empty p-orbital on boron is oriented toward the gold center (torsion angle = 92.7°), analogous to the reported complex **A** (Figure 1).[6a] The different backbone of **3′** (C_1 linker) compared to the C_2 bridge in **A** results in a larger B1−Au1 distance (3.18 Å vs A: 2.663(8) Å), which would lead to a much weaker Z-type interaction.

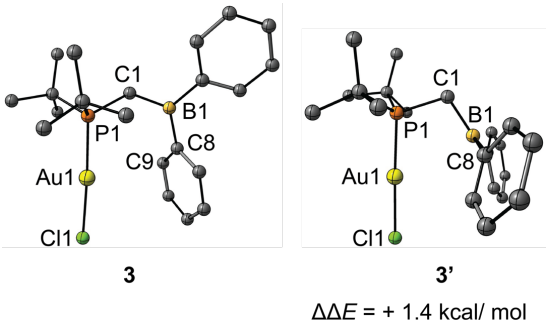

Figure 2. Two optimized geometries for compound **3** (hydrogens are omitted for clarity). Selected bond lengths (Å) and angles (°) **3**: P1−Au1 2.28, B1−Au1 3.94, C8−Au1 3.50, C9−Au1 3.28, P1−Au1−Cl1 176.9, P1−C1−B1 119.0, P1−C1−B1−C8 53.8. **3′**: P1−Au1 2.28, B1−Au1 3.18, P1−Au1−Cl1 177.1, P1−C1−B1 106.4, P1−C1−B1−C8 92.7.

The minor product of the reaction was identified as a result of double addition of phosphinoborane **2** to (Me_2S)AuCl and concomitant cleavage of the gold−chloride bond forming bisligated zwitterionic complex **4** (Scheme 3), which compares well with complex **E** that is obtained with P/Al analogue **1** (Scheme 1).[8a] Colorless crystals suitable for X-ray diffraction were obtained by slow vapor diffusion of *n*-hexane into a solution of **4** in tetrahydrofuran (THF). The molecular structure of gold complex **4** (Scheme 3) revealed a slightly bent P1−Au1−P2 bond angle (169.11(3)°) and remarkably similar P−C−B bond angles (121.0(2)° and 120.9(2)°). The closest aryl−gold distance is Au1−C7 (3.798(3) Å), suggesting the absence of any π-interaction, and the B2−Au1 distance of 4.175(4) Å reveals no Z-type interaction. The side product **4** can be synthesized and isolated in 82% yield by the reaction of an excess (6 equiv) of ambiphilic ligand **2** with (Me_2S)AuCl in DCM. The $^{31}P\{^1H\}$ NMR spectrum of **4** revealed only one signal as a singlet at 80.5 ppm at room temperature, which splits at −50 °C into two broad singlets at 79.6 and 78.6 ppm. At −50 °C, still no signal was observed in the $^{11}B\{^1H\}$ NMR spectrum, indicating a fast exchange of the chloride atom between the Lewis acidic boron sites.

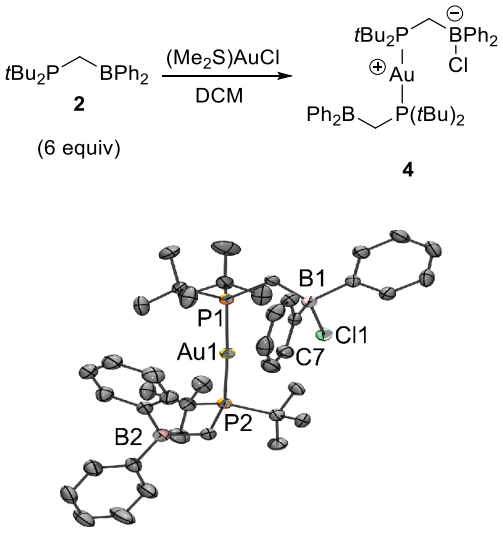

Scheme 3. Formation of bis-ligated complex **4** (top) and the molecular structure (bottom) of **4** (ellipsoids are set at 50% probability, hydrogens are omitted for clarity). Selected bond lengths (Å) and angles (°): P1–Au1 2.3387(8), P2–Au1 2.3217(8), Cl1–Au1 3.2522(8), C7–Au1 3.798(3), B1–Au1 3.863(4), B2–Au1 4.175(4), B1–Cl1 1.961(3), P1–Au1–P2 169.11(3), P1–C1–B1 121.0(2), P2–C22–B2 120.9(2), Σ(CB1C) 337.1, Σ(CB2C) 359.5.

Interestingly, the ambiphilic P/B- and P/Al-based ligands **1** and **2** react differently with sulfur-based gold(I) chlorides; therefore, we systematically evaluated all possible coordination modes (**I**−**IV**; Scheme 4). In the first case, the sulfur-based ligand is displaced by the ambiphilic ligand (**I**), which was found for phosphinoborane **2** (Scheme 2), with the possibility of additional interaction of the boron moiety of the ligand with the liberated sulfur ligand (**II**). Another possibility is that the ambiphilic ligand facilitates cleavage of the gold−chloride bond to afford compound **III**, which is unstable and can be stabilized at the cationic gold(I) center by the sulfur-based ligand (**IV**), which was reported for phosphinoalane **1** (Scheme 1).

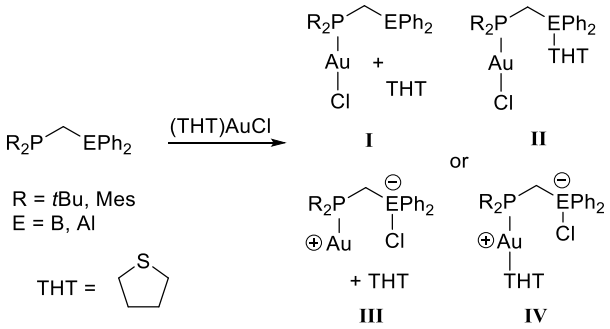

Scheme 4. Computational analysis of the various coordination modes of C_1-bridged ligands.

To gain more insights into the distinct reactivity of ambiphilic ligands **1** and **2**, we resorted to DFT calculations at the ωB97X−D/6-31G* (Def2-QZVP for Au) level of theory[28] and investigated the influence of P substituents (R = *t*Bu, Mes) and Lewis acids (B, Al) on the reaction, using a methylene linker as a common C_1 bridge between the Lewis acid and the base.[29] In accordance with our experimental data, phosphinoborane **2** (R = *t*Bu, E = B, Scheme 2) favors coordination mode **I** (ΔE = −32.1 kcal/mol). Additional interaction of the complex with THT (mode **II**) is weak ($\Delta\Delta E_{\mathbf{I–II}}$ = −12.9 kcal/mol) and entropically disfavored ($\Delta\Delta G_{\mathbf{I–II}}$ = 4.6 kcal/mol). Exchange of the relatively strong Au−Cl bond for the weaker B−Cl bond (mode **III**) is highly disfavored ($\Delta\Delta E_{\mathbf{I–III}}$ = 37.6 kcal/mol), which could be compensated by Au−THT bond formation (mode **IV**, $\Delta\Delta E_{\mathbf{III–IV}}$ = −45.8 kcal/mol), albeit this stabilization is insufficient to account for the entropy effect ($\Delta\Delta G_{\mathbf{I–IV}}$ = 7.7 kcal/mol) and prevents the formation of complex **IV**. Interestingly, changing the Lewis acid from boron to aluminum had a large impact on the relative stabilities (R = *t*Bu, E = Al, Scheme 4). Cleavage of the Au−Cl bond becomes less endothermic ($\Delta\Delta E_{\mathbf{I–III}}$ = 17.3 kcal/mol) because of the formation of a stronger Al−Cl bond compared to the B−Cl bond (approx. 21 kcal/mol stronger). Additional stabilization by THT makes coordination mode **IV** now the most favorable complex (ΔE = −68.1 kcal/mol; ΔG = −51.3 kcal/mol),[30] which explains the distinct difference in reactivity between a P/B and P/Al ambiphilic ligand and is fully consistent with the formation of complex **3** (Scheme 2) and **D** (Scheme 1). The influence of the P substituents is in both cases very limited, resulting in the same trend for the mesityl-substituted phosphinoborane (R = Mes, E = B) with a preference for coordination mode **I** and

phosphinoalane (R = Mes, E = Al) that prefers heterolytic cleavage of the gold−chloride bond (**IV**).[31] These findings illustrate that for these geminal Lewis acid/base pairs, the P substituent has a modest influence on the preferred coordination mode, whereas the nature of the Lewis acid is decisive and thus is an important design element for the development of ambiphilic ligands for the coordination chemistry and catalysis.

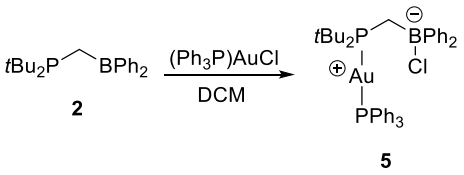

Scheme 5. Gold−chloride cleavage by phosphinoborane **2**.

To further explore the reactivity of phosphinoborane **2** toward gold(I) complexes, we also used $(Ph_3P)AuCl$ that bears the stronger donating triphenylphosphine ligand. Slow addition of a solution of **2** in DCM to a solution of $(Ph_3P)AuCl$ in DCM at 0 °C resulted in a clean conversion to a new product **5** (Scheme 5). $^{31}P\{^1H\}$ NMR spectroscopy revealed two doublets (AB system, 79.6 and 43.9 ppm, $J_{P,P}$ = 305 Hz), indicating that both ligand **2** and triphenylphosphine are coordinated to the gold(I) metal center in a linear fashion. The $^{11}B\{^1H\}$ NMR chemical shift of 3.1 ppm is the characteristic for a quaternary boron center. Colorless crystals suitable for the X-ray diffraction analysis were obtained by layering a saturated solution of **5** in toluene with pentane at room temperature (Figure 3).

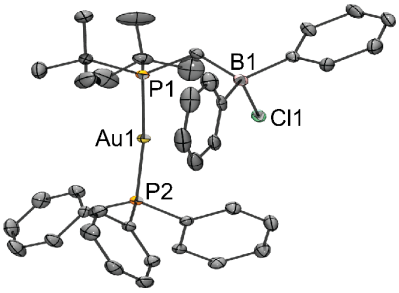

Figure 3. Molecular structure of compound **5** (ellipsoids are set at 50% probability; hydrogens and a pentane molecule are omitted for clarity). Selected bond lengths (Å) and angles (°): P1−Au 2.3251(7), P2−Au 2.2974(7), P1−Au−P2 173.71(3), Au−Cl 3.2386(8), B−Cl 1.971(3), Σ(CB1C) 335.8.

The molecular structure of **5** displays that both triphenylphosphine and phosphinoborane **2** are coordinated to gold in an almost linear fashion (P−Au−P 173.71(3)°). Remarkably, the chloride atom is transferred to the borane moiety of the ligand and, with a Au−Cl distance of 3.2386(8) Å, any Au−Cl interaction is excluded. Pyramidalization around the boron center (Σ(CBC) = 336°) because of the formation of a chloroborate is in accordance with the strong upfield ^{11}B NMR chemical shift. To the best of our knowledge, **2** is the first example of a bidentate phosphinoborane ambiphilic ligand to cleave a gold−chloride bond.

To verify the role of the Lewis acid in the gold−chloride bond cleavage, we resorted to DFT calculations at the *ω*B97X−D/6-31G* (Def2-QZVP for Au) level of theory.[28] These calculations showed that ligation of phosphinoborane **2** to (Ph_3P)AuCl initially affords the neutral Y-shaped complex **6** (Figure 4), a geometry which could not be located on the potential energy surface when using (THT)AuCl.[32,33] Subsequently, the pendent borane of intermediate **6** is able to abstract the chloride from the gold center to form product **5** (ΔE = −35.2 kcal/mol, ΔG = −18.5 kcal/mol), which is favored over the formation of the linear Au(I)Cl complex **3** (ΔE = −9.12 kcal/mol, ΔG = −9.17 kcal/mol) by dissociation of PPh_3 from intermediate **6**.

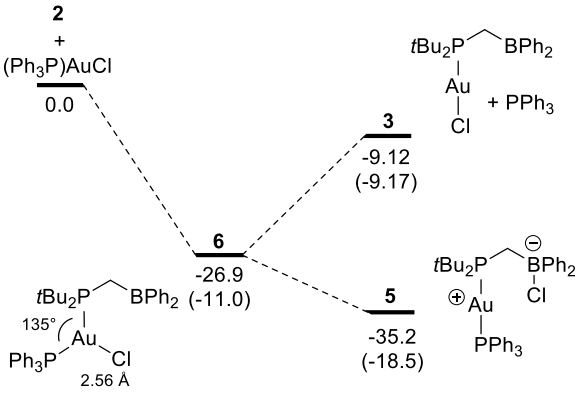

Figure 4. Energy and (Gibbs free energy) profile calculated for the gold−chloride bond cleavage by phosphinoborane **2**. The relative energies are given in kcal/mol.

The distinct difference in reactivity of **2** with (Me_2S)AuCl and (Ph_3P)AuCl, forming **3** and **5**, respectively, can be directly related to the difference in bond strength of the Au−Cl

and B−Cl bond and to the stabilization by the coligand (SMe_2 or PPh_3) of the different coordination modes (Scheme 4). When ligand **2** is reacted with $(Me_2S)AuCl$, the SMe_2 coligand does not bind strongly enough to gold to compensate the formation of the weak B−Cl bond and to facilitate the Au−Cl bond cleavage, and therefore **2** only displaces the weakly bound sulfur ligand. In contrast, when **2** is reacted with $(Ph_3P)AuCl$, the triphenylphosphine coligand is more strongly bound to gold (approximately 18 kcal/mol stronger compared to THT) and is thereby able to compensate for the formation of the weaker B−Cl, leading to the cleavage of the Au−Cl bond, which emphasizes the diverse reactivity of **2** as ambiphilic ligand.

4.3 Conclusion

Linear phosphine gold(I) chloride complex **3** can be obtained by the reaction of ambiphilic ligand **2** with $(Me_2S)AuCl$. The side product of this reaction was identified as bisligated complex **4** and can be isolated by reacting an excess of ligand **2** with $(Me_2S)AuCl$. The distinct difference in reactivity between the geminal P/Al-based ligand **1** and its P/B-analogue **2** toward sulfur-based gold(I) precursors was studied by DFT calculations, which revealed that the nature of the Lewis acid determines the preference for ligand displacement versus gold−chloride abstraction. Changing $(Me_2S)AuCl$ for triphenylphosphine gold chloride drastically changed the outcome of the reaction with ambiphilic ligand **2**, which forms complex **5** by the cleavage of the gold−chloride bond, instead of the displacement of PPh_3. To the best of our knowledge, the geminal phosphinoborane **2** is the first example of a P/B ambiphilic ligand that is capable of cleaving a gold−chloride bond.

4.4 Experimental Section

All manipulations were carried out under an atmosphere of dry nitrogen, using standard Schlenk and drybox techniques, and were performed in the dark as precaution to prevent decomposition. Solvents were purified, dried and degassed according to standard procedures. ^{1}H and $^{13}C\{^{1}H\}$ NMR spectra were recorded on a Bruker Avance 400 and internally referenced to the residual solvent resonances (CD_2Cl_2: ^{1}H δ 5.32, $^{13}C\{^{1}H\}$ δ 53.8). $^{31}P\{^{1}H\}$

and $^{11}B\{^{1}H\}$ NMR spectra were recorded on a Bruker Avance 400 and externally referenced (85% H_3PO_4, $BF_3{\cdot}OEt_2$, respectively). Mass spectra were collected on an AccuTOF GC v 4g, JMS-T100GCV Mass spectrometer (JEOL, Japan). FD Emitter, Carbotec or Linden (Germany), FD 10 µm. Current rate 51.2 mA/min over 1.2 min. Typical measurement conditions are: Counter electrode –10kV, Ion source 37V. Melting points were measured in sealed capillaries and are uncorrected. *t*$Bu_2PCH_2BPh_2$ (**2**) was prepared following a literature procedure,[20a] $(Me_2S)AuCl$ and $(Ph_3P)AuCl$ were purchased from Sigma Aldrich and used without any further purification.

Preparation of compound 3:

A solution of *t*$Bu_2PCH_2BPh_2$ (**2**; 0.100 g, 0.31 mmol, 1.00 equiv) in DCM (5 mL) was added dropwise to a solution of $(Me_2S)AuCl$ (0.091 g, 0.31 mmol, 1.00 equiv) in DCM (5 mL) at 0 °C. Next, the reaction mixture was warmed to room temperature and a colorless solution with a purple precipitate was obtained. The reaction mixture was filtered and dried *in vacuo*. The obtained white solids were washed with *n*-pentane (3 x 4 mL) and dried *in vacuo* to yield a pale purple solid (0.130 g, 75% purity based on $^{31}P\{^{1}H\}$ NMR spectroscopy). Colorless X-ray quality crystals were grown at room temperature by vapor diffusion of *n*-pentane into a solution of **3** in DCM.

^{1}H NMR (400.13 MHz, CD_2Cl_2, 297 K): δ 7.77 (d, $^{3}J_{H,H}$ = 7.4 Hz, 4H; *o*-Ph*H*), 7.58 (t, $^{3}J_{H,H}$ = 7.4 Hz, 2H; *p*-Ph*H*), 7.49 (t, $^{3}J_{H,H}$ = 7.4 Hz, 4H; m-Ph*H*), 2.58 (d, $^{2}J_{H,P}$ = 15.5 Hz, 2H; PCH_2B), 1.36 (d, $^{3}J_{H,P}$ = 15.2 Hz, 18H; P$(CH_3)_3$).

^{13}C{^{1}H} NMR (100.62 MHz, CD_2Cl_2, 298 K): δ 141.2 (only observed in the HMBC spectrum, $^{2}J_{C,H}$ coupling with *o*-Ph*H*, $^{3}J_{C,H}$ coupling with m-Ph*H* and PCH_2B; *ipso*-Ph*C*), 136.4 (s; *o*-Ph*C*), 132.5 (s; *p*-Ph*C*), 128.6 (s; *m*-Ph*C*), 36.5 (d, $^{1}J_{C,P}$ = 27.1 Hz; P$C(CH_3)_3$), 29.9 (d, $^{2}J_{C,P}$ = 5.7 Hz; P$(CCH_3)_3$), 17.0 (only observed in the HSQC spectrum, $^{1}J_{C,H}$ coupling with PCH_2B; PCH_2B).

^{31}P{^{1}H} NMR (162.0 MHz, CD_2Cl_2, 297 K): δ 75.3 (s).

^{11}B{^{1}H} NMR (128.4 MHz, CD_2Cl_2, 297 K): δ 70.2 (br. s).

Preparation of compound 4:

A solution of (Me_2S)AuCl (0.040 g, 0.115 mmol, 1.00 equiv) in DCM (5 mL) was quickly added to a solution of tBu$_2$PCH$_2$BPh$_2$ (**2**; 0.224 g, 0.69 mmol, 6.00 equiv) in DCM (6 mL). Subsequently, the reaction mixture was stirred for 10 minutes after which the solvent was removed *in vacuo*. The obtained pale white solids were washed with *n*-pentane (3 x 5 mL) and dried *in vacuo* to yield a pale white solid (0.83 g, 82 %). Colorless X-ray quality crystals were obtained by vapor diffusion of *n*-hexane into a solution of **4** in THF.

^{1}H NMR (400.13 MHz, CD_2Cl_2, 297 K): δ 7.70 (d, $^3J_{H,H}$ = 7.6 Hz, 8H; *o*-Ph*H*), 7.28–7.21 (m, 12H; *m*,*p*-Ph*H*), 2.24 (br. t, 4H; PC*H*$_2$B), 1.22 (t, $^3J_{H,P}$ = 7.2 Hz, 18H; PC(C*H*$_3$)$_3$).

^{13}C{^{1}H} NMR (100.62 MHz, CD_2Cl_2, 298 K): δ 135.0 (s; *o*-Ph*C*), 127.7 (s; *m*-Ph*C*), 36.8 (t, $^1J_{C,P}$ = 11.5 Hz; P*C*(CH$_3$)$_3$), 30.3 (t, $^2J_{C,P}$ = 3.2 Hz; PC(*C*H$_3$)$_3$) 18.1 (only observed in the HSQC spectrum, $^1J_{C,H}$ coupling with PC*H*$_2$B; P*C*H$_2$B), the signals for *p*-Ph*C* and *ipso*-Ph*C* are unresolved).

^{31}P{^{1}H} NMR (162.0 MHz, CD_2Cl_2, 297 K): δ 80.5 (s).

^{11}B{^{1}H} NMR (128.4 MHz, CD_2Cl_2, 297 K): not observed due to fast chloride exchange between the boron atoms.

HR-MS (FD): 845.40609 $[M - Cl]^+$, calcd for $C_{42}H_{60}Au_1B_2P_2$ 845.40219.

Melting point (nitrogen, sealed capillary): 129 °C (decomp.).

Preparation of compound 5:

A solution of tBu$_2$PCH$_2$BPh$_2$ (**2**; 0.055 g, 0.17 mmol, 1.00 equiv) in DCM (4 mL) was added dropwise to a solution of (Ph$_3$P)AuCl (0.084 g, 0.17 mmol, 1.00 equiv) in DCM (5 mL) at 0 °C. Subsequently, the reaction mixture was warmed to room temperature and stirred for 30 minutes after which the solvent was removed *in vacuo*. The obtained white solids were washed with *n*-pentane (3 x 4 mL) and dried *in vacuo* to yield **5** as a white solid (0.121 g, 87%). Colorless X-ray quality crystals were grown by layering a saturated solution of **5** in toluene with *n*-pentane at room temperature.

^{1}H NMR (400.13 MHz, CD_2Cl_2, 297 K): δ 7.64–7.51 (m, 15H; PPh*H*), 7.47 (m, 4H; B*m*-Ph*H*), 6.93 (m, 6H; B*o*-Ph*H*, B*p*-Ph*H*), 1.77 (d, $^2J_{H,P}$ = 13.6 Hz, 2H; PC*H*$_2$B), 1.21 (d, $^3J_{H,P}$ = 14.0 Hz, 18H; PC(C*H*$_3$)$_3$).

$^{13}C\{^1H\}$ NMR (100.62 MHz, CD_2Cl_2, 299 K): δ 156.8 (only observed in the HMBC spectrum, $^2J_{C,H}$ coupling with *o*-Ph*H* and PC*H*$_2$B; *ipso*-Ph*C*), 134,7 (d, $J_{C,P}$ = 13.9 Hz; *o*- or *m*-PPh*C*), 133.5 (s, *m*-Ph*C*), 132.1 (d, $^4J_{C,P}$ = 2.3 Hz; *p*-PPh*C*), 130.2 (d, $^1J_{C,P}$ = 52.5 Hz; *ipso*-PPh*C*), 129.7 (d, $J_{C,P}$ = 11.2 Hz; *o*- or *m*-PPh*C*), 126.7 (s, *o*-Ph*C*), 124.4 (s, *p*-Ph*C*), 36.0 (d, $^1J_{C,P}$ = 22.5 Hz; P*C*(CH$_3$)$_3$), 30.6 (d, $^2J_{C,P}$ = 5.5 Hz; PC(*C*H$_3$)$_3$), 19.3 (only observed in the HSQC spectrum, $^1J_{C,H}$ coupling with PC*H*$_2$B; P*C*H$_2$B).

$^{31}P\{^1H\}$ NMR (162.0 MHz, CD_2Cl_2, 297 K): δ 79.6 (d, $^2J_{P,P}$ = 304.5 Hz), 43.9 (d, $^2J_{P,P}$ = 304.5 Hz).

$^{11}B\{^1H\}$ NMR (128.4 MHz, CD_2Cl_2, 297 K): δ 3.1 (br. s).

HR-MS (FD): 783.27866 $[M - Cl]^+$, calcd for $C_{39}H_{45}Au_1B_1P_2$ 783.27550.

Melting point (nitrogen, sealed capillary): 143 °C (decomp.)

VT NMR spectroscopy of compound 4:

A solution of compound **4** in dichloromethane-d_2 (0.55 mL) was loaded into an NMR tube. Of this sample, the $^{31}P\{^1H\}$ NMR spectrum was recorded using a Brucker Avance 300 at room temperature, -50°C and back at room temperature (Figure 5).

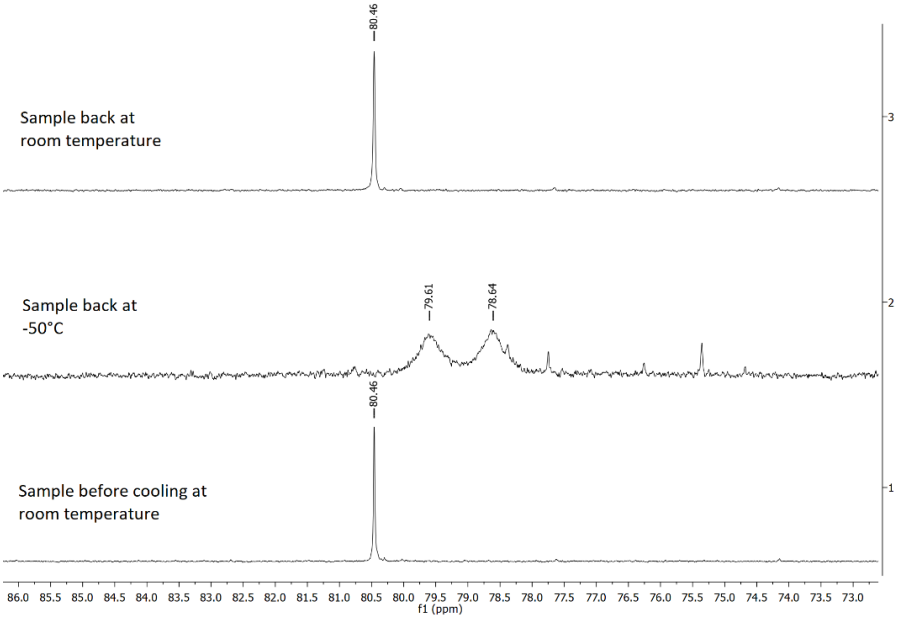

Figure 5. VT $^{31}P\{^1H\}$ spectra (121.5 MHz, CD_2Cl_2) recorded of **4**.

Computational Details:

All structures were optimized at the ωB97X−D[34] level of theory, using Gaussian 09, Revision D01.[28] Geometry optimizations were performed using the 6-31G(d) basis set[35,36] (Def2-QZVP for Au)[37] and the nature of each stationary point was confirmed by frequency calculations.

Comprehensive overview on computational study P/B vs. P/Al

Reaction of *t*Bu$_2$PCH$_2$BPh$_2$ with (THT)AuCl

Table 1. Energy and Gibbs free energy for the reaction of (THT)AuCl with *t*Bu$_2$PCH$_2$BPh$_2$.

	ΔE (kcal/mol)	ΔG (kcal/mol)
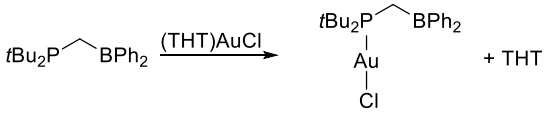	–32.06	–28.95
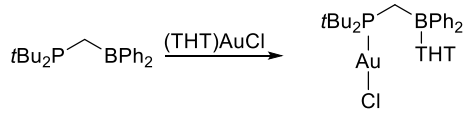	–44.99	–24.39
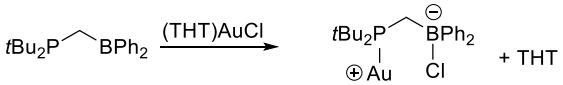	+5.52	+9.43
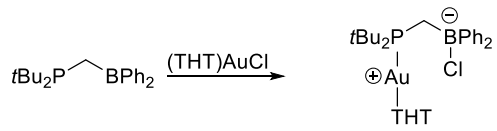	–40.24	–21.24
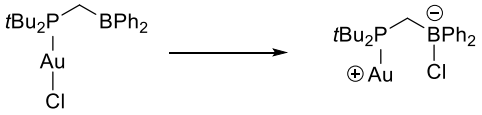	+37.58	+38.38

Reaction of tBu$_2$PCH$_2$AlPh$_2$ with (THT)AuCl

Table 2. Energy and Gibbs free energy for the reaction of (THT)AuCl with tBu$_2$PCH$_2$AlPh$_2$.

		ΔE (kcal/mol)	ΔG (kcal/mol)
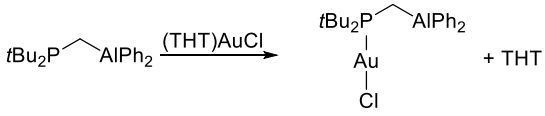		–32.27	–28.75
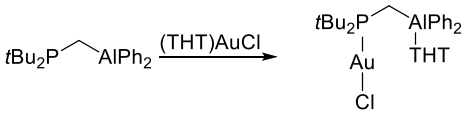		–61.30	–43.35
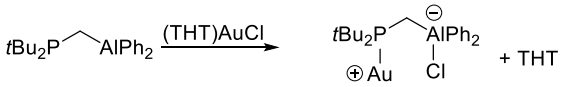		–14.99	–9.60
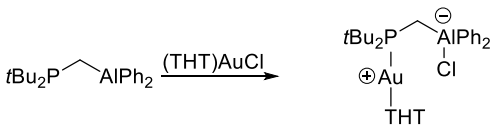		–68.05	–51.33
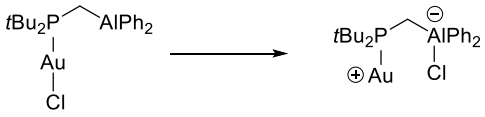		+17.28	+19.14

Reaction of $Mes_2PCH_2BPh_2$ with (THT)AuCl

Table 3. Energy and Gibbs free energy for the reaction of (THT)AuCl with $Mes_2PCH_2BPh_2$.

		ΔE (kcal/mol)	ΔG (kcal/mol)
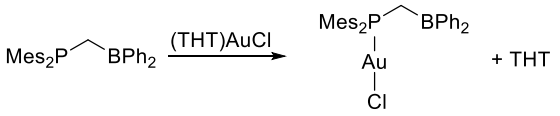		–19.74	–18.58
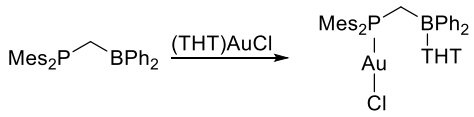		–37.51	–17.66
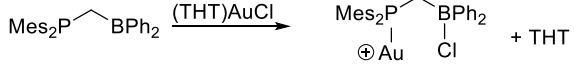		+12.72	+17.64
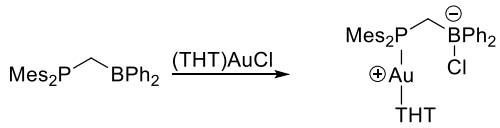		–34.92	–16.94
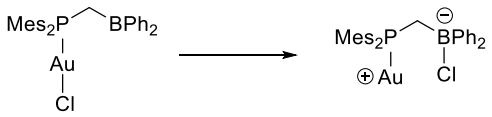		+32.46	+36.22

Reaction of $Mes_2PCH_2AlPh_2$ with (THT)AuCl

Table 4. Energy and Gibbs free energy for the reaction of (THT)AuCl with $Mes_2PCH_2AlPh_2$.

	ΔE (kcal/mol)	ΔG (kcal/mol)
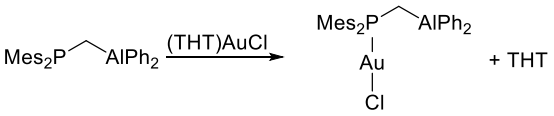	–26.99	–22.46
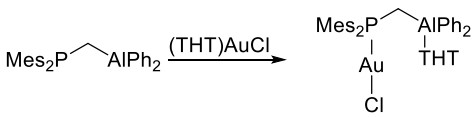	–48.54	–30.14
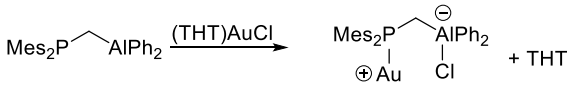	–2.18	–0.67
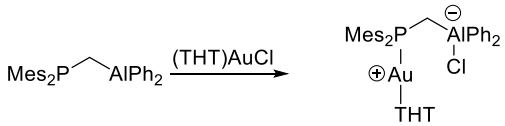	–55.83	–37.73
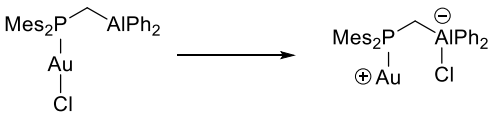	+24.81	+21.79

X-ray crystal structure determinations of 3, 4 and 5:

The single-crystal X-ray diffraction stdy were carried out on an Agilent SuperNova Single source diffractometer with Eos detector at 173(2) K using Mo-Kα radiation (λ= 0.71073Å) (**3**, **4**) or a Bruker D8 Venture diffractometer with Photon100 detector at 123(2) K using Mo-Kα radiation (λ = 0.71073 Å) (**5**). Patterson Methods (**3**, **4**) or Direct Methods (**5**) (SHELXS-97) were used for structure solution[38] and refinement[39] was carried out using SHELXL-

2014 (full-matrix least-squares on F^2). Hydrogen atoms were localized by difference electron density determination and refined using a riding model. Semi-empirical absorption corrections were applied. For **3** and **5** an extinction correction were applied.

3: colorless crystals, $C_{21}H_{30}AuBClP$, M_r = 556.64, crystal size 0.50 × 0.30 × 0.20 mm, monoclinic, space group $P2_1/c$ (No. 14), a = 17.0948(3) Å, b = 7.0396(1) Å, c = 17.6526(3) Å, β = 91.814(1)°, V = 2123.26(6) Å^3, Z = 4, ρ = 1.741 Mg/m^{-3}, μ(Mo-K$_\alpha$) = 7.131 mm^{-1}, F(000) = 1088, $2\theta_{max}$ = 55.0°, 9206 reflections, of which 4870 were independent (R_{int} = 0.032), 227 parameters, R_1 = 0.035 (for 4333 I > 2σ(I)), wR_2 = 0.082 (all data), S = 1.07, largest diff. peak / hole = 3.030 / -1.939 e Å^{-3}.

4: colorless crystals, $C_{42}H_{60}AuB_2ClP_2$, M_r = 880.87, crystal size 0.30 × 0.20 × 0.10 mm, monoclinic, space group $C2/c$ (No. 15), a = 28.3351(8) Å, b = 11.3935(3) Å, c = 27.0950(7) Å, β = 112.237(3)°, V = 8096.7(4) Å^3, Z = 8, ρ = 1.445 Mg/m^{-3}, μ(Mo-K$_\alpha$) = 3.807 mm^{-1}, F(000) = 3584, $2\theta_{max}$ = 59.8°, 20333 reflections, of which 10254 were independent (R_{int} = 0.031), 433 parameters, R_1 = 0.032 (for 8564 I > 2σ(I)), wR_2 = 0.073 (all data), S = 1.04, largest diff. peak / hole = 1.117 / -1.192 e Å^{-3}.

5: colorless crystals, $C_{39}H_{45}AuBClP_2 \cdot C_5H_{12}$, M_r = 891.06, crystal size 0.12 × 0.08 × 0.02 mm, orthorhombic, space group $Pbca$ (No. 61), a = 19.0712(8) Å, b = 18.7238(7) Å, c = 23.2135(10) Å, V = 8289.2(6) Å^3, Z = 8, ρ = 1.428 Mg/m^{-3}, μ(Mo-K$_\alpha$) = 3.720 mm^{-1}, F(000) = 3616, $2\theta_{max}$ = 55.2°, 170457 reflections, of which 9537 were independent (R_{int} = 0.064), 443 parameters, 24 restraints, R_1 = 0.027 (for 7454 I > 2σ(I)), wR_2 = 0.056 (all data), S = 1.08, largest diff. peak / hole = 1.650 / -0.921 e Å^{-3}.

CCDC 1572409 (**3**), 1572410 (**4**), and 1572411 (**5**) contain the supplementary crystallographic data for this paper. These data can be obtained free of charge from The Cambridge Crystallographic Data Centre via www.ccdc.cam.ac.uk/data_request/cif.

4.5 References

[1] G. Bouhadir, A. Amgoune, D. Bourissou, *Adv. Organomet. Chem.* **2010**, *58*, 1−107.

[2] F. -G. Fontaine, J. Boudreau, M.-H. Thibault, *Eur. J. Inorg. Chem.* **2008**, 5439−5454.

[3] G. Bouhadir, D. Bourissou, Coordination of Lewis acids to transition metals: Z-type ligands. *The Chemical Bond III*; Springer International Publishing, **2016**; pp 141−201.

[4] G. Bouhadir, D. Bourissou, *Chem. Soc. Rev.* **2016**, *45*, 1065−1079.

[5] M. Devillard, G. Bouhadir, D. Bourissou, *Angew. Chem. Int. Ed.* **2015**, *54*, 730−732.

[6] For bidentate ligands see: (a) S. Bontemps, G. Bouhadir, K. Miqueu, D. Bourissou, *J. Am. Chem. Soc.* **2006**, *128*, 12056−12057. For tridentate ligands see: (b) M. Sircoglou, S. Bontemps, M. Mercy, N. Saffon, M. Takahashi, G. Bouhadir, L. Maron, D. Bourissou, *Angew. Chem. Int. Ed.* **2007**, *46*, 8583−8586. For tetradentate ligands, see: c) S. Bontemps, G. Bouhadir, W. Gu, M. Mercy, C.-H. Chen, B. M. Foxman, L. Maron, O. V. Ozerov, D. Bourissou, *Angew. Chem. Int. Ed.* **2008**, *47*, 1481–1484. d) M. Sircoglou, S. Bontemps, G. Bouhadir, N. Saffon, K. Miqueu, W. Gu, M. Mercy, C.-H. Chen, B. M. Foxman, L. Maron, O. V. Ozerov, D. Bourissou, *J. Am. Chem. Soc.* **2008**, *130*, 16729–16738. e) J. W. Taylor, A. McSkimming, M.-E. Moret, W. H. Harman, *Angew. Chem. Int. Ed.* **2017**, *56*, 10413–10417.

[7] For a carbon-boron based bidentate ambiphilic ligand, see: M. Toure, O. Chuzel, J. L. Parrain, *Dalton Trans.* **2015**, *44*, 7139–7143.

[8] For bidentate ligands, see: a) M. Devillard, E. Nicolas, C. Appelt, J. Backs, S. Mallet-Ladeira, G. Bouhadir, J. C. Slootweg, W. Uhl, D. Bourissou, *Chem. Commun.* **2014**, *50*, 14805–14808. b) M. Devillard, E. Nicolas, A. W. Ehlers, J. Backs, S. Mallet-Ladeira, G. Bouhadir, J. C. Slootweg, W. Uhl, D. Bourissou, *Chem. Eur. J.* **2015**, *21*, 74–79. For tridentate ligands, see: c) M. Sircoglou, G. Bouhadir, N. Saffon, K. Miqueu, D. Bourissou, *Organometallics* **2008**, *27*, 1675–1678. For tetradentate ligands see: d) M. Sircoglou, N. Saffon, K. Miqueu, G. Bouhadir, D. Bourissou, *Organometallics* **2013**, *32*, 6780–6784.

[9] M. Sircoglou, M. Mercy, N. Saffon, Y. Coppel, G. Bouhadir, L. Maron, D. Bourissou, *Angew. Chem. Int. Ed.* **2009**, *48*, 3454–3457.

[10] For tridentate ligands see: a) J. Backs, M. Lange, J. Possart, A. Wollschläger, C. Mück-Lichtenfeld, W. Uhl, *Angew. Chem. Int. Ed.* **2017**, *56*, 3094–3097. For tetradentate ligands, see: b) E. J. Derrah, M. Sircoglou, M. Mercy, S. Ladeira, G. Bouhadir, K. Miqueu, L. Maron, D. Bourissou, *Organometallics* **2011**, *30*, 657–660.

[11] C. Tschersich, C. Limberg, S. Roggan, C. Herwig, N. Ernsting, S. Kovalenko, S. Mebs, *Angew. Chem. Int. Ed.* **2012**, *51*, 4989–4992.

[12] For tridentate ligands, see: a) P. Gualco, T. P. Lin, M. Sircoglou, M. Mercy, S. Ladeira, G. Bouhadir, L. M. Pérez, A. Amgoune, L. Maron, F. P. Gabbaï, D. Bourissou, *Angew. Chem. Int. Ed.* **2009**, *48*, 9892–9895. b) P. Gualco, M. Mercy, S. Ladeira, Y. Coppel, L. Maron, A. Amgoune, D. Bourissou, *Chem. Eur. J.* **2010**, *16*, 10808–10817. For tetradentate ligands, see: c) P. Gualco, S. Mallet-Ladeira, H. Kameo, H. Nakazawa, M. Mercy, L. Maron, A. Amgoune, D. Bourissou, *Organometallics* **2015**, *34*, 1449–1453.

[13] For bidentate ligands, see: a) J. S. Jones, F. P. Gabbaï, *Chem. Eur. J.* **2017**, *23*, 1136–1144. For tridentate ligands, see: b) H. Yang, F. P. Gabbaï, *J. Am. Chem. Soc.* **2015**, *137*, 13425–13432. For a review on ambiphilic ligands containing antimony, see: c) J. S. Jones, F. P. Gabbaï, *Acc. Chem. Res.* **2016**, *49*, 857–867.

[14] For a zirconium/phosphorus based ambiphilic ligand that can cleave a gold–chloride bond see: S. Büschel, C. Daniliuc, P. G. Jones, M. Tamm, *Organometallics*, **2010**, *29*, 671–675.

[15] a) H. Yang, T. P. Lin, F. P. Gabbaï, *Organometallics*, **2014**, *33*, 4368–4373. For a review on ambiphilic ligands containing tellurium, see: b) J. S. Jones, F. P. Gabbaï, F. P. *Chem. Lett.* **2016**, *45*, 376–384.

[16] One phosphinoborane ambiphilic ligand is reported to cleave a methyl-nickel bond, resulting in the formation of a cationic metal center: A. Fischbach, P. R. Bazinet, R. Waterman, T. D. Tilley, *Organometallics* **2008**, *27*, 1135–1139.

[17] D. W. Stephan, *Science* **2016**, *354*, 1248.

[18] D. W. Stephan, *Acc. Chem. Res.* **2015**, *48*, 306−316.

[19] D. W. Stephan, G. Erker, *Angew. Chem. Int. Ed.* **2010**, *49*, 46–76.

[20] a) F. Bertini, V. Lyaskovskyy, B. J. J. Timmer, F. J. J. de Kanter, M. Lutz, A. W. Ehlers, J. C. Slootweg, K. Lammertsma, *J. Am. Chem. Soc.* **2012**, *134*, 201–204; b) E. R. M. Habraken, L. C. Mens, M. Nieger, M. Lutz, A. W. Ehlers, J. C. Slootweg, *Dalton Trans*. **2017**, *46*, 12284–12292.

[21] D. H. A. Boom, A. W. Ehlers, M. Nieger, J. C. Slootweg, *Z. Naturforsch., B: Chem. Sci.* **2017**, *72*, 781–784.

[22] Same reactivity was observed when (THT)AuCl was used as gold(I) metal precursor. However, the selectivity was lower compared to (Me_2S)AuCl and the formation of several unidentified products was observed by $^{31}P\{^1H\}$ NMR spectroscopy, therefore (Me_2S)AuCl was solely used as sulfur-based metal precursor.

[23] Compound **3** is unstable in solution over time. A solution of **3** in DCM slowly degrades at room temperature into unidentifiable products observed by $^{31}P\{^1H\}$ NMR spectroscopy, as well as insoluble purple solids.

[24] For geometry around d10 Au(I) metal centers see: M. A. Carvajal, J. J. Novoa, S. Alvarez, *J. Am. Chem. Soc.* **2004**, *126*, 1465−1477.

[25] Comparable parallel alignment of a mesityl group was found in a (iPr$_2$P-oC$_6$H$_4$-BMes$_2$)PdCl(allyl) complex, see: S. Bontemps, G. Bouhadir, D. C. Apperley, P. W. Dyer, K. Miqueu, D. Bourissou, D. *Chem. Asian J.* **2009**, *4*, 428–435.

[26] D. V. Partyka, T. J. Robilotto, M. Zeller, A. D. Hunter, T. G. Gray, *Organometallics* **2008**, *27*, 28–32.

[27] D. V. Partyka, M. P. Washington, J. B. Updegraff III, R. A. Woloszynek, J. D. Protasiewics, *Angew. Chem. Int. Ed.* **2008**, *47*, 7489–7492.

[28] M. J. Frisch, G. W. Trucks, H. B. Schlegel, G. E. Scuseria, M. A. Robb, R. J. Cheeseman, G. Scalmani, V. Barone, B. Mennucci, G. A. Petersson, H. Nakatsuji, M. Caricato, X. Li, H. P. Hratchian, A. F. Izmaylov, J. Bloino, G. Zheng, J. L. Sonnenberg, M. Hada, M. Ehara, K. Toyota, R. Fukuda, J. Hasegawa, M. Ishida, T. Nakajima, Y. Honda, O. Kitao, H. Nakai, T. Vreven, J. A. Montgomery, Jr., J. E. Peralta, F. Ogliaro, M. Bearpark, J. J. Heyd, E. Brothers, K. N. Kudin, V. Staroverov, T. Keith, R. Kobayashi, J. Normand, K. Raghavachari, A. Rendell, J. C. Burant, S. S. Iyengar, J. Tomasi, M. Cossi, N. Rega, J. M. Millam, M. Klene, J. E. Knox, J. B. Cross, V. Bakken, C. Adamo, J. Jaramillo, R. Gomperts, R. E. Stratmann, O. Yazyev, A. J. Austin, R. Cammi, C. Pomelli, J. W. Ochterski, R. L. Martin, K. Morokuma, V. G. Zakrzewski, G. A. Voth,

P. Salvador, J. J. Dannenberg, S. Dapprich, A. D. Daniels, O. Farkas, J. B. Foresman, J. V. Ortiz, J. Cioslowski, D. J. Fox, *Gaussian 09, Revision D.01*; Gaussian, Inc.: Wallingford, CT, 2004.

[29] We used (THT)AuCl as a metal precursor for our computational study because the reactivity of phosphinoalane **1** with (THT)AuCl was already well-described, and ligand **2** reacts with (THT)AuCl and (Me_2S)AuCl in a similar fashion.

[30] This observation compares well with the findings of Bourissou and co-workers for tridentate ambiphilic ligands, see ref 8c.

[31] For a comprehensive overview of the computational analysis including the effect of the phosphorus substituents, see the Experimental Section.

[32] M. C. Gimeno, A. Laguna, *Chem. Rev.* **1997**, *97*, 511−522.

[33] For X-ray structures of neutral Y-shaped gold(I)chloride complexes, see: a) M. Khan, C. Oldham, G. T. Tuck, *Can. J. Chem.* **1981**, *59*, 2714−2718. b) C. Khin, A. S. A. Hashimi, F. Rominger, *Eur. J. Inorg. Chem.* **2010**, 1063–1069. c) S. K. Mohapatra, S. Büschel, C. Daniliuc, P. G. Jones, M. Tamm, *J. Am. Chem. Soc.* **2009**, *131*, 17014−17023.

[34] J.-D. Chai,; M. Head-Gordon, M. *Phys. Chem. Chem. Phys.* **2008**, *10*, 6615–6620.

[35] a) R. Ditchfield, W. J. Hehre, J. A. Pople, *J. Chem. Phys.* **1971**, *54*, 724–728. b) W. J. Hehre, R. Ditchfield, J. A. Pople, *J. Chem. Phys.* **1972**, *56*, 2257–2261. c) P. C. Hariharan, J. A. Pople, *Theor. Chem. Acc.* **1973**, *28*, 213–222. d) P. C. Hariharan, J. A. Pople, *Mol. Phys.* **1974**, 27, 209–214. e) M. S. Gordon, *Chem. Phys. Lett.* **1980**, *76*, 163–168. f) M. M. Francl, W. J. Pietro, W. J. Hehre, J. S. Binkley, D. J. DeFrees, J. A. Pople, M. S. Gordon, *J. Chem. Phys.* **1982**, *77*, 3654–3665. g) R. C. Binning, Jr., L. A. Curtiss, *J. Comp. Chem.* **1990**, *11*, 1206–1216. h) J.-P. Blaudeau, M. P. McGrath, L. A. Curtiss, L. Radom, *J. Chem. Phys.* **1997**, *107*, 5016–5021. i) V. A. Rassolov, J. A. Pople, M. A. Ratner, T. L. Windus, *J. Chem. Phys.* **1998**, *109*, 1223–1229. j) V. A. Rassolov, M. A. Ratner, J. A. Pople, P. C. Redfern, L. A. Curtiss, *J. Comp. Chem.* **2001**, *22*, 976–984.

[36] For the polarization functions, see: M. J. Frisch, J. A. Pople, J. S. Binkley, *J. Chem. Phys.* **1984**, *80*, 3265–3269.

[37] a) F. Weigend, R. Ahlrichs, *Phys. Chem. Chem. Phys.* **2005**, *7* , 3297–3305. b) F. Weigend, *Phys. Chem. Chem. Phys.* **2006**, *8*, 1057–1065.

[38] G. M. Sheldrick, *Acta Crystallogr.* **2008**, *A64*, 112–122.

[39] G. M. Sheldrick, *Acta Crystallogr.* **2015**, *C71*, 3–8.